Neutral meson and direct photon measurements with the ALICE experiment

Oleksandr Kovalenko

National Centre for Nuclear Research, Warsaw, Poland

May 17, 2019

Outline

- Introduction
- ALICE setup
- Neutral mesons
  - Measurement techniques
  - pp, p-Pb, Pb-Pb spectra
- Direct photons in Pb-Pb
  - Definitions
  - Spectra per centrality bin
- Summary

Introduction

- Study QCD phase diagram
- Investigate properties of hot ($T \sim 10^{12}$ K) and dense nuclear matter
- Chiral symmetry restoration and the deconfinement (transition from quark to hadronic matter) mechanisms
- Search for QGP phase and measure its properties

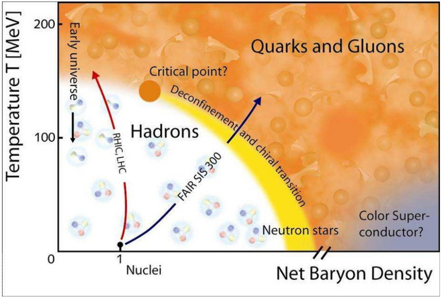

Why neutral mesons

Meson production in pp should be described by pQCD at large transverse momentum

- Constrain model parameters of perturbative (NLO, NNLO) and non-perturbative regimes (parton distribution function, fragmentation function)
- Test scaling laws
- Main input for direct photon analysis
- Can be identified in a wider p_{T} range than charged mesons

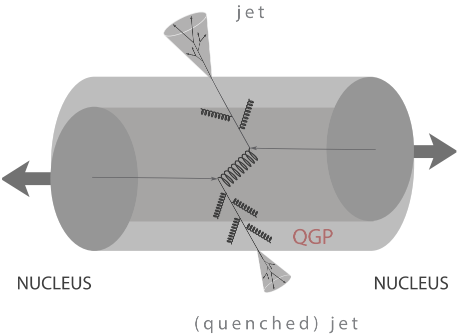

Direct photons

Inclusive photons

- Decay photons
  - Decay photons coming from π^0, η, ω, etc.
  - The largest contribution
- Prompt photons
  - Produced in hard scatterings of quark and gluons
  - Mostly contribute at high transverse mometnum $p_{\mathrm{T}} \gtrsim 5$ GeV/c
- Thermal photons
  - Comes from the collision volume
  - Dominates at $p_{\mathrm{T}} \lesssim 3$ GeV/c

Why do we study direct photons?

- Temperature estimation via measurement of p_{T} distribution of thermal photons in Pb-Pb
- Study of the properties of quark-gluon matter
- Direct photons are produced at all stages of the collisions providing an integrated image of the system

ALICE experiment

Detectors for neutral meson reconstruction

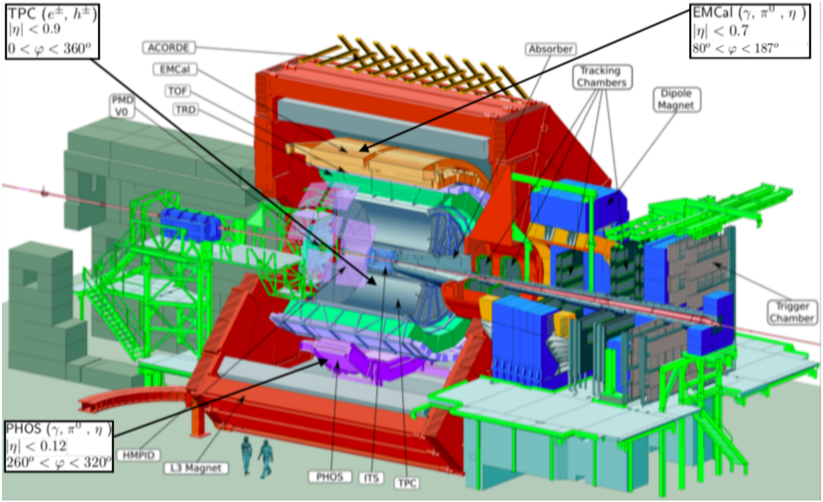

Neutral meson analysis

The neutral mesons can be reconstructed by means of invariant mass analysis

$$M_{\gamma\gamma} = \sqrt{2E_1E_2(1-\cos\theta_{1,2})}$$

- Two gamma channel: hadron $\rightarrow \gamma\gamma$
- Photon conversion (PCM): meson $\rightarrow (\gamma \rightarrow e^+e^-) + (\gamma \rightarrow e^+e^-)$
- Hybrid methods (EMCal + PCM, PHOS + PCM)

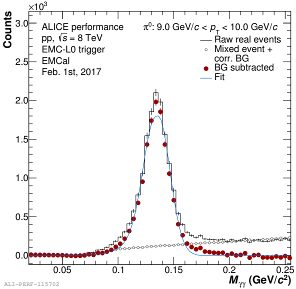

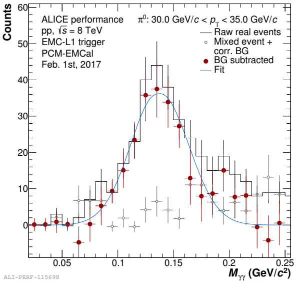

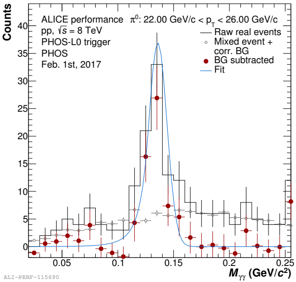

Comparison of detectors

Related paper: EPJC 77 (2017) 339

- The EMC efficiency raises at low p_{T} and decreases above 10 GeV/c due to cluster merging
- The PHOS efficiency is higher than EMC efficiency at $p_{\mathrm{T}} \lesssim 1$ GeV/c
- The PCM-EMC efficiency is approximately 10 times smaller due to the conversion probability
- The decrease in PCM-EMC efficiency is due to shower overlap of EMC photon with one of the conversion legs
- The PCM efficiency affected by probability for both reconstructed photons
- The PCM-EMC method extend measurement to very high transverse momentum ($p_{\mathrm{T}} \sim 40$ GeV/c), by means of identification of merged decays via shower shape method

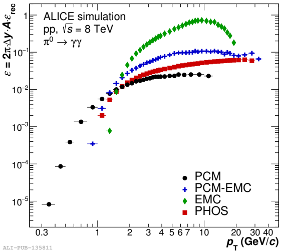

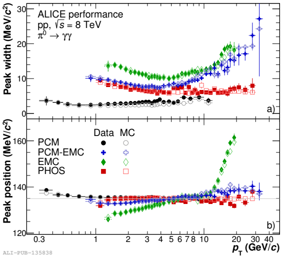

Neutral meson analysis

ALICE is able to measure neutral mesons

- In different systems (pp, p-Pb, Pb-Pb)
- At different collision energies
- Using different methods
- In the wide p_{T} range

The measurements from different methods can be combined giving the wide p_{T} -range of the final spectra

	system	energy	reference
Neutral mesons	pp	0.9, 7 TeV	PLB 717(2012) 162-172
	pp	2.76 TeV	EPJC 74 (2014) 3108
	pp	8 TeV	EPJC 77 (2017) 339
	p-Pb	5.02 TeV	EPJC 78 (2018) 624
	Pb-Pb	2.76 TeV	EPJC 74 (2014) 3108
Direct Photons	pp	2.76, 8 TeV	PRC 99 (2019) 024912
	Pb-Pb	2.76 TeV	PLB 754 (2016) 23-248

π^0 spectra in pp

- π^0 spectra are up to 40 GeV/c for $\sqrt{s} = 2.76$ TeV
- Data shows power law behaviour at high p_T
- PYTHIA 8.2 Monash 2013 describes the data at high p_T
- PYTHIA 8.2 Monash 2013 shows a deviation from the data at moderate p_T at higher energies
- NLO calculations predict 20%-60% higher yield, and the difference increases with p_T

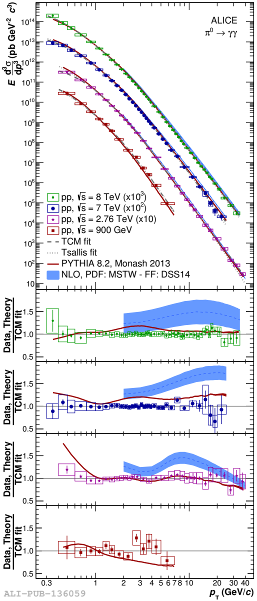

NLO:
PRD 91 (2015) 1, 014035

η spectra in pp

- η spectra are up to 40 GeV/c for $\sqrt{s} = 8$ TeV
- Data follows power law behaviour at high p_{T}
- PYTHIA 8.2 Monasch 2013 shows a deviation from the data at low p_{T} at higher energies
- NLO calculations predict 50%-100% higher yield, and the difference increases with p_{T}

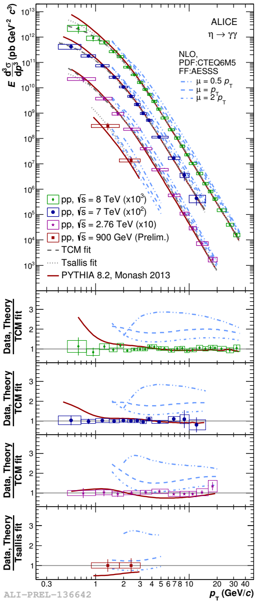

Related papers:

PLB 717(2012) 162-172
EPJC 74 (2014) 3108
EPJC 78 (2018) 263

Neutral meson production in p-Pb

- Both π^0 and η spectra are mesured up to $p_{\mathrm{T}} < 20$ GeV/c
- Various methods for π^0 measurement (PHOS, EMCal, PCM, PCM-EMCal)
- EMCal, PCM, PCM-EMCal measurements for η production
- Well described by Tsallis function

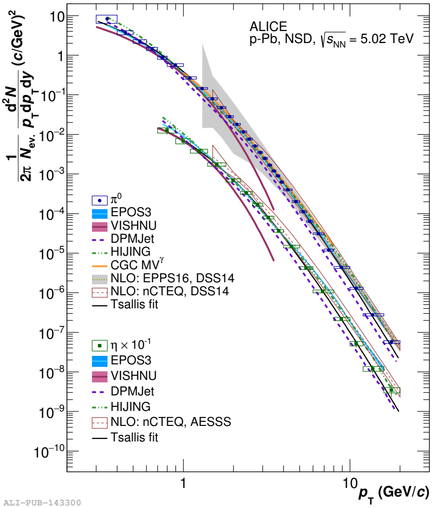

EPJC 78 (2018) 624

Neutral mesons in p-Pb (comparison with models)

- EPOS3 well reproduces π^0 spectrum
- Problems with η at high p_{T} (good description below 3 GeV/c)
- VISHNU shows good description at low p_{T}
- HIJING and DPMJET depart from the data for p_{T} larger than 4 GeV/c, the disagreement increases with p_{T}

Related papers:

EPOS3: K.Werner et al., PRC 89 (2014) 064903
VISHNU: C.Shen at al., PRC 95 (2017) 014906

Related paper: EPJC 78 (2018) 624

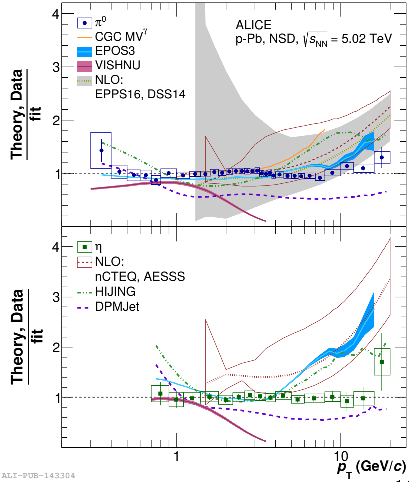

Neutral pion measurements in Pb-Pb

- Based on 2010 data sample
- First measuremnt of π^0 spectrum in Pb-Pb $0.6 < p_{\mathrm{T}} < 12$ GeV/c
- Pb-Pb data can be well described by the Tsallis fits
- pp data at $\sqrt{s} = 2.76$ GeV fitted with power law function at high p_{T}

Related paper:
EPJC 74 (2014) 3108

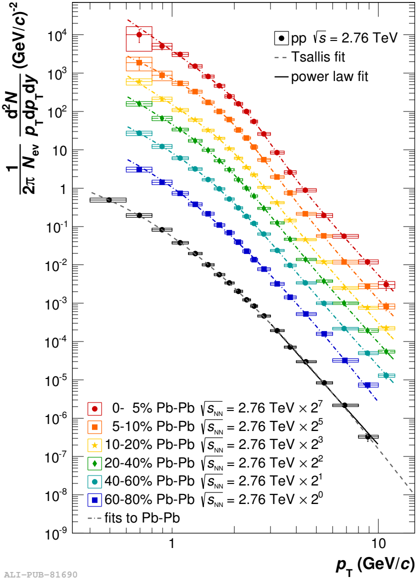

η meson spectra in Pb-Pb

- Increased statistics with 2011 data sample
- First result on η meson spectra in Pb-Pb at the LHC
- The π^0 spectrum extended up to 20 GeV/c
- Good description of the low p_{T} region
- The EQ and NEQ versions of SHM reproduce the shape π^0 spectrum at low p_{T}
- For η NEQ SHM underestimates the yield at the low p_{T} region

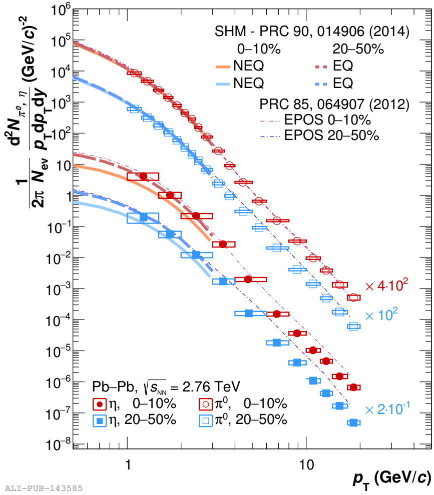

Related paper:

PRC 98 (2018), 044901

Nuclear modification factor

$$R_{\mathrm{AA}} = \frac{d^2 N_{\mathrm{AA}}/dp_{\mathrm{T}}dy}{\langle T_{\mathrm{AA}}\rangle\, d^2\sigma_{\mathrm{pp}}/dp_{\mathrm{T}}dy}$$

where $\langle T_{\mathrm{AA}}\rangle = \langle N_{\mathrm{coll}}\rangle / \sigma_{\mathrm{pp}}$

- $R_{\mathrm{AA}} = 1$ corresponds to the absence of nuclear medium effects
- Observed large suppression $R_{\mathrm{AA}} \sim 0.1$ at 7 GeV/c central events. Ratio increases decreasing centrality
- Agrees with results for charged hadrons
- High p_{T} particle supression reflects parton energy loss (jet-quenching)

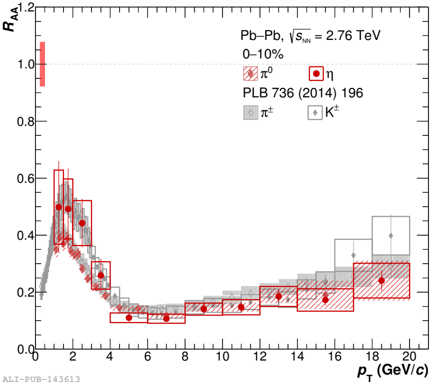

Nuclear modification factor (centrality dependence)

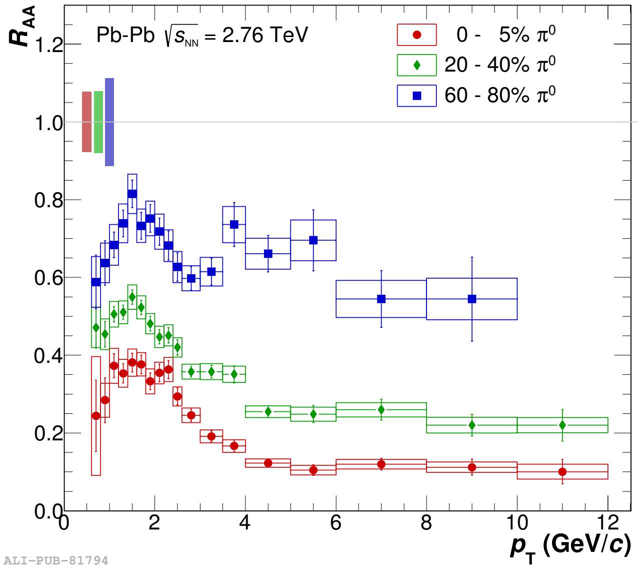

Nuclear modification factor p-Pb

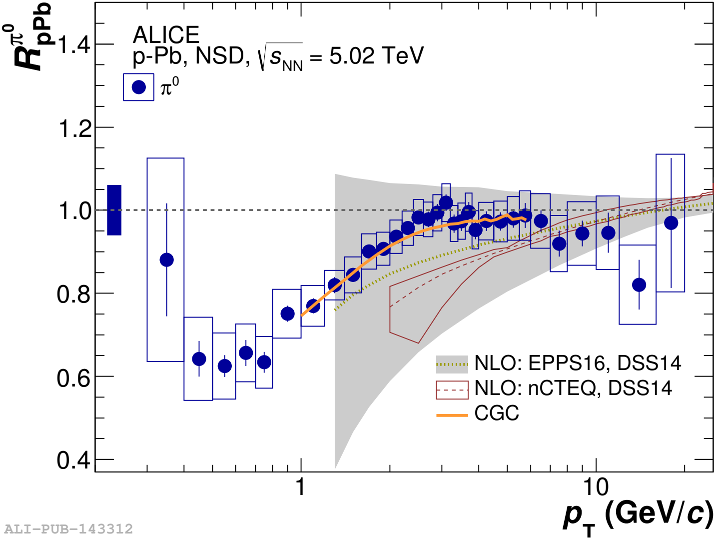

Direct photon measurements

Direct photons:

All photons that are not coming from hadron decays

$$\gamma_{\textsf{direct}} = \gamma_{\textsf{inc}} - \gamma_{\textsf{decay}} = (1 - 1/R_\gamma)\,\gamma_{\textsf{inc}}$$

where $R_\gamma = \gamma_{\textsf{inc}}/\gamma_{\textsf{decay}}$

Double Ratio

$$R_{\textsf{double}} \sim \frac{\gamma_{\textsf{inc}}/{\pi^0}_{\textsf{par}}}{\gamma_{\textsf{decay}}/{\pi^0}_{\textsf{MC}}} \sim R_\gamma$$

Values of R_γ greater than unity indicate the direct photon signal.

Double ratio in Pb-Pb

- Three centrality ranges in $0.9 < p_{\mathrm{T}} < 14$ GeV/c
- Compared with JETPHOX and pQCD calculations
- Visible excess of photons (compared to NLO pQCD) at $p_{\mathrm{T}} < 4$ GeV/c in central collisions

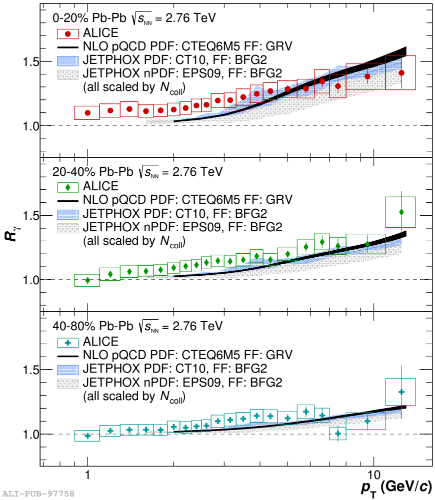

Related paper:

PLB 754 (2016) 23-248

Direct photons in Pb-Pb

Related paper:
PLB 754 (2016) 23-248

Different level of agreement for different models, for the central collisions:

- *Chatterjee et al.*: 2+1 hydro, fluctuating initial conditions, $\tau_0 = 0.14$ fm/c, $\langle T_{\text{init}}^{0-20\%} \rangle = 740$ MeV.
- *v. Hees et al.*: ideal hydro with initial flow, $\tau_0 = 0.2$ fm/c, $\langle T_{\text{init}}^{0-20\%} \rangle = 682$ MeV,
- *Paquet et al.*: 2+1 viscous hydro with IP-GLASMA initial conditions, $\tau_0 = 0.14$ fm/c, $\langle T_{\text{init}}^{0-20\%} \rangle = 385$ MeV,
- *Linnyk et al.*: off-shell transport, microscopic description of evolution,
- Exponential fit for $p_{\text{T}} < 2.2$ GeV/c inv. slope $T_{\text{eff}} = 304 \pm 11$ stat $\pm\, 40$ sys MeV, which is an estimate of real collision energy, but it doesn't take into account the expanding medium

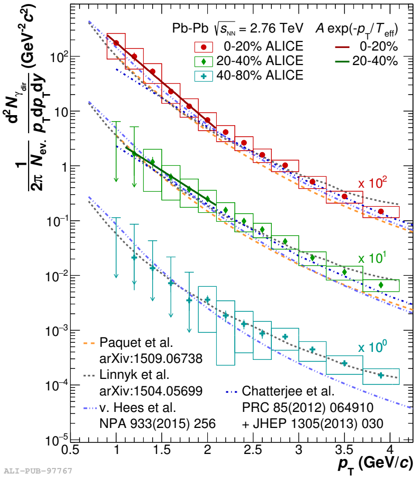

Summary

- ALICE has measured neutral mesons in a wide p_{T} range
- The measurements allow testing of the parton distribution and fragmentation functions
- The double ratio ($R_\gamma > 1$) in central Pb-Pb collisions exceeds the prompt photon pQCD predictions below 4 GeV/c
- Various models with QGP formation show different levels of agreement with the measurement
- The inverse slope of direct photon spectrum in central Pb-Pb collisions is ~ 300 MeV

backup slides

Nuclear modification factor, energy dependence

- Clear centrality dependence
- Central collisions lead to more significant effects
- Modification factor decreases with energy (more medium effects at higher energies)

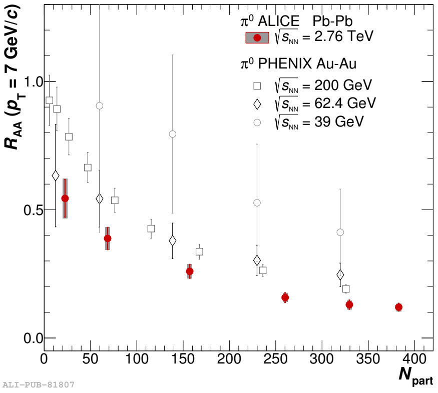

PHOS

- Modular detector
- Consists of $4 \times 64 \times 56$ $PbWO_4$ crystals
- Crystal size 2.2 cm $\times$ 2.2 cm $\times$ 18 cm
- Acceptance: $250^o < \varphi < 320^o$, $|\eta| < 0.13$
- 4.6 m to the interaction point

EMCal and DCal

- 76 layers of scintillator detector, 20 supermodules
- Channel size 6 cm $\times$ 6 cm $\times$ 24.6 cm
- Acceptance (EMCal): $80^o < \varphi < 187^o$, $|\eta| < 0.7$
- Acceptance (DCal):
  $260^o < \varphi < 320^o$, $0.22 < |\eta| < 0.7$,
  $320^o < \varphi < 327^o$, $\eta < 0.7$
- 4.28 m to the interaction point

Tracking system

Time projection chamber (TPC)

- Barrel shape, with $d = 5$ m, $r = 5$ m
- Acceptance:($0 < \varphi < 2\pi$, $|\eta| < 0.9$
- Readout chambers 72
- Electrode 100 kV

Inner tracking system (ITS)

- 2 layers of pixel detectors (SPD)
- 2 layers of drift detectors (SDD)
- 2 layers of strip detectors (SSD)
- Acceptance: $0 < \varphi < 2\pi$, $|\eta| < 0.9$

Centrality in Pb-Pb

Centrality clases are defined based on the fractions of Pb-Pb cross-section:

- Charged particle multiplicity in VZERO detector
- Energy deposited in Forward calorimeter ZDC
- Glauber MC, makes correspondance between impact parameter b, and number of binary collision N_{coll} and number of participants N_{part}
- Particle multiplicity per independent source of particles ("ancestors") is modelled by NBD

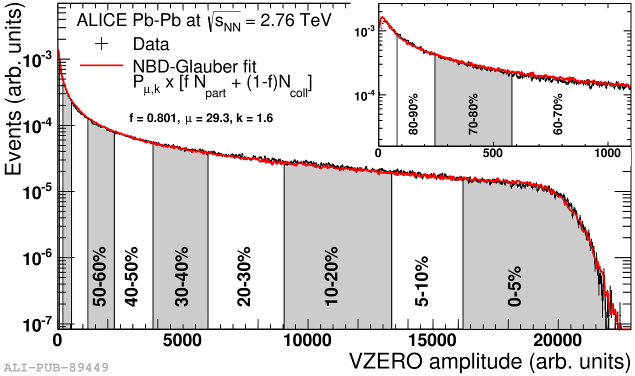

Functions

Tsallis:

$$E\frac{d^3\sigma^{pp\to\pi^0+X}}{dp^3} \sim \frac{\sigma_{\mathrm{pp}}^{\mathrm{INEL}}}{2\pi}A\frac{(n-1)(n-2)}{nC\left(nC+m(n-2)\right)}\left(1+\frac{m_{\mathrm{T}}-m}{nC}\right)^{-n}$$

Hagedorn:

$$E\frac{d^3\sigma^{pp\to\pi^0+X}}{dp^3} \sim \left(\frac{p_0}{p_0-p_{\mathrm{T}}}\right)^{n}$$

Power law:

$$E\frac{d^3\sigma^{pp\to\pi^0+X}}{dp^3} \sim C{p_{\mathrm{T}}}^{-n}$$

Two component model:

$$E\frac{d^3\sigma^{pp\to\pi^0+X}}{dp^3} \sim A_c\exp\left(E_{\mathrm{T,kin}}/T_{\mathrm{e}}\right)+A\left(1+\frac{{p_{\mathrm{T}}}^2}{nT^2}\right)^{-n}$$

Decay photon contributions